

Robust Control of the Classic Dynamic Ball and Beam System

Javier Jiménez-Cabas[1], Farid Meléndez-Pertuz[1], Luis David Díaz-Charris[1], Carlos Collazos-Morales[2(✉)], and Ramón E. R. González[3(✉)]

[1] Departamento de Ciencias de la Computación y Electrónica, Universidad de la Costa, Barranquilla, Colombia
fmelendel@cuc.edu.co
[2] Vicerrectoría de Investigaciones, Universidad Manuela Beltrán, Bogotá, Colombia
cacollazos@gmail.com
[3] Departamento de Física, Universidad Federal de Pernambuco, Recife, Brazil
ramayo_g@yahoo.com.br

Abstract. This article presents the design of robust control system for the Ball and Beam system, as well as the comparison of their performances with classic control techniques. Two controllers were designed based on Algebraic Riccati Equations for the synthesis of H_2 and H_∞ controllers and a third one based on Linear Matrix Inequalities techniques for the design of H_∞ controllers. The results show that H_∞ controllers offer better performance.

Keywords: Robust control H_2 and H_∞ · Uncertainties · Modeling · Ball and beam system

1 Introduction

One of the central topics of discussion in the design of feedback control systems has been the robustness of these systems in the presence of uncertainties, which is the reason of the development of methods to tackle the problem of robust control, has become one of the areas of most active research since the 1970s [1–3].

Several researches have yielded as a result a variety of methods that employ different mathematical techniques [4, 5] extending the field of application of robust control theory to different areas such as the control of chemical processes, control of power systems and the investigation of feedback mechanisms in biological systems, giving great importance to make more contributions in this topic.

In this sense, the ball and beam system has become one of the most popular laboratory models used in the teaching of control engineering [6]. Its main importance is because of is a simple system to understand and is also unstable in open loop, which allows studying both classic and modern control techniques, while analyzing the benefits of each one.

Therefore, this paper shows the synthesis of the robust controllers for the ball and beam system, as well as the verification of their operation and the comparison of their

© Springer Nature Switzerland AG 2020
O. Gervasi et al. (Eds.): ICCSA 2020, LNCS 12251, pp. 134–144, 2020.
https://doi.org/10.1007/978-3-030-58808-3_11

performance of their controls with the classic control techniques. Two devices were designed using solution techniques of Algebraic Riccatis Equations (ARE) for the synthesis of H_2 y H_∞ controls and a third one based on Linear Matrix Inequalities (LMI) techniques for the design of H_∞ controllers. The results shown that the H_∞ results offer better performance.

To verify the operation of the designed systems, the module Ball and Beam from Quanser® was used.

2 Ball and Beam System Description

The module Ball AND Beam from Quanser® (Fig. 1) [7] that was used is made up of a steel bar in parallel with a resistor, which make up the path on which a metal ball travels freely.

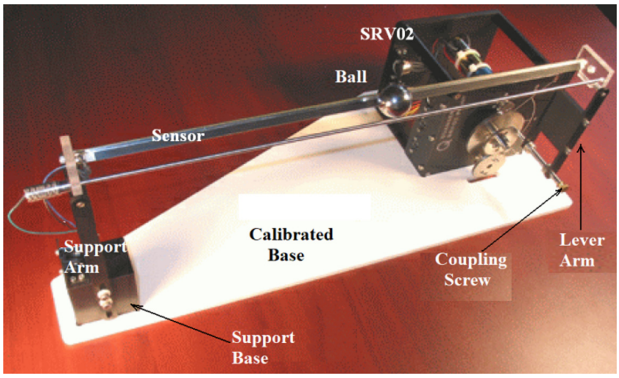


Fig. 1. Ball and beam system attached to the plant SRV02 (Quanser®).

When the ball moves over the path it acts similar to the brush on a potentiometer. The position of the ball is obtained by measuring the voltage on the steel bar. By coupling this system with the SRV02 (from the same manufacturer), a DC motor drives the bar and the motor angle controls the inclination of the steel bar.

The objective is to design a control system that allows the position of the ball to track a reference signal. The manufacturer provides a control system based on two PD loops which is taken as a reference to compare the performances obtained with the robustly designed control systems.

2.1 Mathematical Model

Figure 2 shows the Ball and Beam system [8]. A translational force (due to gravity) and a rotational force (due to the torque produced by its angular acceleration) act on the ball. The first of these forces is given by:

$$F_{tx} = mg \sin \alpha \tag{1}$$

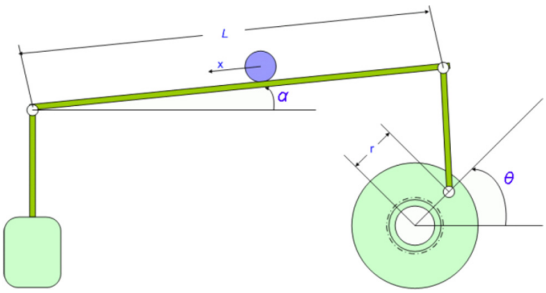


Fig. 2. Ball and Beam System diagram.

The torque produced by the rotational movement of the ball is equal to the radius of the ball multiplied by the rotational force. Using Newton's second law, there is possible to write:

$$T_r = F_{rx}R = Ja = J\frac{\ddot{x}}{R} \tag{2}$$

Taking into account that the moment of inertia of the ball is $J = (2/5)\, mR^2$ (where m is the mass of the ball), it yields:

$$F_{rx} = {}^{2}/_{5}\, m\ddot{x} \tag{3}$$

Applying Newton's second law to the ball:

$$m\ddot{x} = F_{tx} - F_{rx} = mg \sin \alpha - {}^{2}/_{5} m\ddot{x} \tag{4}$$

Then,

$$\ddot{x} = {}^{5}/_{7}\, g \sin \alpha \tag{5}$$

On the other hand, it has been defined ***Arc*** as the arc traveled by the lever arm, measuring the angles in radians, then it is possible to obtain:

$$Arc = \theta r = \alpha L \tag{6}$$

Now, there is obtained the model of the position SRV02 [9]. Initially the electrical components of the motor are considered, Fig. 3 shows the schematic diagram of the armature circuit.

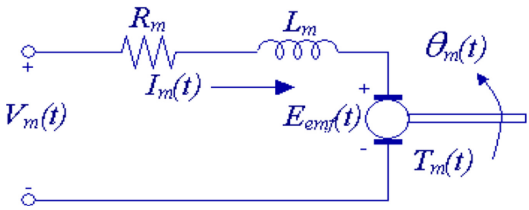


Fig. 3. DC Motor armature circuit.

Applying Kirchhoff's voltage law we obtain:

$$V_m - R_m I_m - L_m \frac{dI_m}{dt} - E_{emf} = 0 \tag{7}$$

Considering that $L_m << R_m$

$$I_m = \frac{V_m - E_{emf}}{R_m} \tag{8}$$

where, E_{emf} is proportional to the motor shaft angular velocity w_m, hence:

$$I_m = \frac{V_m - K_m \dot{\theta}_m}{R_m} \tag{9}$$

Aiming to consider the mechanical aspects of the motor there is important to apply Newton's second law on the motor shaft,

$$J_m \ddot{\theta}_m = T_m - \frac{T_l}{\eta_g K_g} \tag{10}$$

where $T_l / \eta_g K_g$ is the torque of the load seen through the pinions and η_g is the efficiency of the gear box. Now applying Newton's second law to motor load, the next equation emerges:

$$J_l\ddot{\theta}_l = T_l - B_{eq}\dot{\theta}_l \tag{11}$$

where B_{eq} is the viscous coefficient of friction seen at the outlet. Substituting (10) in (11), it becomes

$$J_l\ddot{\theta}_l = \eta_g K_g T_m - \eta_g K_g J_m \ddot{\theta}_m - B_{eq}\dot{\theta}_l \tag{12}$$

Noting that $\theta_m = K_g\theta_l$ y $T_m = \eta_m K_t I_m$ (where η_m is the engine efficiency), can be rewritten (12) as:

$$J_l\ddot{\theta}_l + \eta_g K_g^2 J_m \ddot{\theta}_l + B_{eq}\dot{\theta}_l = \eta_g \eta_m K_g K_t I_m \tag{13}$$

Substituting (8) into (13):

$$\begin{aligned} J_{eq}R_m\ddot{\theta}_l + \left(B_{eq}R_m + \eta_g\eta_m K_m K_t K_g^2\right)\dot{\theta}_l \\ = \eta_g\eta_m K_t K_g V_m \end{aligned} \tag{14}$$

where $J_{eq} = J_l + \eta_g J_m K_g^2$. This can be interpreted as the equivalent moment of inertia of the motor system seen from the output.

The complete model of the system is made up of the Eqs. (5), (6) and (14). Table 1 shows the system parameters [7, 9].

Table 1. System parameters.

Symbol	Description	Value	Unities	Variation
L	Beam length	42.5	cm	
R	Ball radius	2.54	cm	
R	Lever arm offset	2.54	cm	
M	Ball mass	0.064	Kg	
G	Gravitational constant	9.8	m/s^2	
K_t	Torque constant	0.0077	N·m	±12%
K_m	*emf* constant	0.0077	V/(rad/s)	±12%
K_g	Total Ratio of Pine Nuts	70		
R_m	Armature Resistance	2.6	Ω	±12%
J_{eq}	J engine equivalent	2×10^{-3}	$Kg{\cdot}m^2$	±10%
B_{eq}	B equivalent	2×10^{-3}	N·m/(rad/s)	±20%
η_g	Gear box efficiency	0.85		±10%
η_m	Engine efficiency	0.69		±5%

3 System Control Design

To achieve that the ball position tracks a reference signal, a control system was designed implementing two independent control loops [8], an internal loop to control the position of the servo axis and an external loop to control the position of the ball on the bar, manipulating the position of the servo. Figure 4 shows the manufacturer's suggested control configuration for both loops.

The feedback status gains given by the manufacturer for both the internal control loop and the external control loop are Kp = 11.1206 V/rad, Kv = 0.11106 V/rad/s and Kp_bb = 0.0017619 rad/cm, Kv_bb = 0.0022433 rad/cm/s respectively.

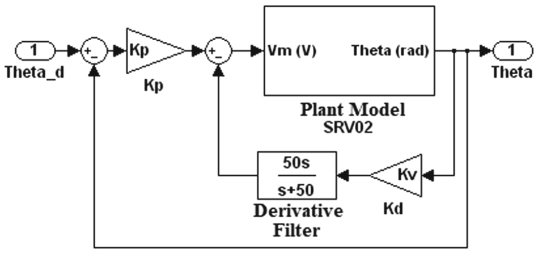


Fig. 4. Control configuration.

For our design, the topology of two control loops was maintained, but using output feedback. The linear models used in each case for the design are as follows.

$$G_m(s) = \left[\begin{array}{cc|c} 0 & 1 & 0 \\ 0 & -35.0427 & 61.6326 \\ \hline 1 & 0 & 0 \end{array}\right] \tag{15}$$

$$G_b(s) = \left[\begin{array}{cc|c} 0 & 1 & 0 \\ 0 & 0 & 0.4179 \\ \hline 100 & 0 & 0 \end{array}\right] \tag{16}$$

3.1 Controllers

To obtain the controllers, unstructured multiplicative uncertainties were considered upon entry into both control loops. Figure 5 shows the block diagram of the closed loop system in which the weights of uncertainties have been included W_i, performance W_d, control signal W_u and desired response W_f.

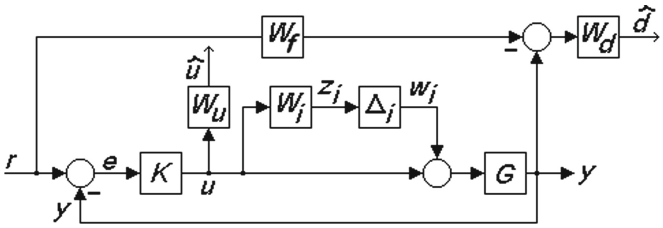


Fig. 5. Close loop system block diagram.

The weight transfer functions used are shown in Table 2.

Table 2. Weights used in the design.

	Internal loop	External loop
W_i	$\frac{0.6394s + 6.648}{s + 39.89}$	1.72×10^{-3}
W_d	$\frac{0.01s + 0.001}{s + 1 \times 10^{-6}}$	$\frac{1 \times 10^{-4}s + 1 \times 10^{-6}}{s + 1 \times 10^{-9}}$
W_f	$\frac{492.8}{s^2 + 39.96s + 492.8}$	$\frac{9}{s^2 + 5.4s + 9}$
W_u	$\frac{s + 157.1}{1 \times 10^{-6}s + 314.2}$	$\frac{s + 100}{1 \times 10^{-9}s + 500}$

The system block diagram is rearranged in the form of the configuration *Δ–P–K* (Fig. 6) for robust controller design [4] and [5].

Below are the controllers obtained for each loop. It should be noted that all of them met the conditions of robust stability and performance in their respective systems.

Controllers H_∞ obtained via method of solution AREs [1–5]. (It should be noted that for instance 1.5e5 = 1.5×10^5).

$$K_m(s) = \left[\begin{array}{ccccccc|c} 548.2 & 1 & 0 & 12e-4 & 0 & -7e-4 & -7e-4 & -62e3 \\ 15e4 & -35 & 28e3 & 0.3 & -2e-4 & -0.2 & -0.2 & 17e6 \\ -23.1 & -0.5 & -309.1 & -1 & -2.1 & 0.5 & -0.1 & 0 \\ -79e-4 & 0 & 0 & 0 & 0 & -0.1 & -0.1 & -403.8 \\ 0 & 0 & 81.3 & 0 & -40 & 0 & 0 & 0 \\ -2 & 0 & 0 & 3e-4 & 0 & -6.6 & -16.5 & -226.4 \\ -5.7 & 0 & 0 & -8e-4 & 0 & 16.5 & -33.3 & -643.5 \\ \hline 0 & 0 & 4 & 0 & 0 & 0 & 0 & 0 \end{array}\right]$$

$$K_b(s) = \left[\begin{array}{cccccc|c} -136.8 & 1 & 0 & 0 & 0 & 0 & -48e3 \\ -9.4e3 & 0 & 681.1 & 0 & 0 & 0 & -33e5 \\ -0.9 & -0.6 & -104.2 & 22e-4 & 11e-4 & -4e-4 & 0 \\ 3e-4 & 0 & 0 & 0 & 1e-3 & 1e-3 & 137.9\ 0 \\ -0.7 & 0 & 0 & 0 & -0.9 & -2.2 & -240.9 \\ -1.2 & 0 & 0 & 0 & 2.2 & -4.5 & -415.6 \\ \hline 0 & 0 & 46.2e-3 & 0 & 0 & 0 & 0 \end{array}\right]$$

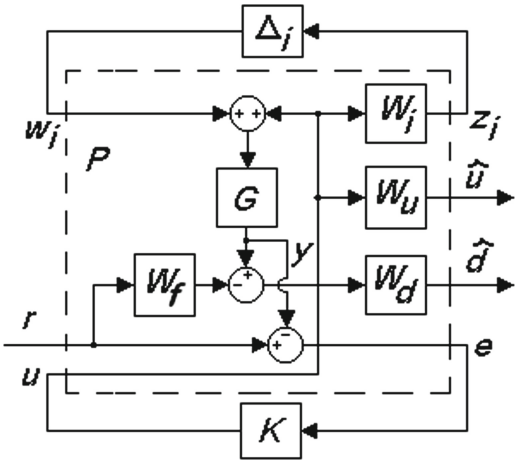


Fig. 6. Configuration *Δ–P–K*.

Controllers H_∞ based on LMI [10–12].

$$K_m(s)=\left[\begin{array}{cccccccc}
-0.2 & 8.5 & -1.2 & 1.4 & -179e-4 & 2.7 & 0.3 & -5.4 \\
8.8 & -418.8 & 59.3 & -56.1 & 7.2 & -57.7 & -36.4 & 435.8 \\
-1.4 & 55.9 & -41.7 & 8.2 & -16.8 & 13.2 & 5.8 & -64.3 \\
1.2 & -67.7 & 10.4 & -46.7 & 6.9 & 50.9 & -1.9 & 65.6 \\
-0.36 & 21.8 & 13.5 & 1.8 & -10 & -30.2 & 6.2 & -17.9 \\
2 & -41.3 & 4.2 & -14.1 & -31.3 & -400 & 89.7 & 69.8 \\
-51.6 & 2583.1 & -393.8 & 360.3 & -82.1 & 93.6 & -561 & -26e2 \\
\hline
1.4 & 60.8 & -10.1 & -9.5 & -33.6 & -389 & 3e-4 & 0
\end{array}\right]$$

$$K_b(s)=\left[\begin{array}{cccccccc}
-31e-3 & -1.7 & -0.8 & 24e-3 & -55e-4 & -36e-4 & -14e-3 & \\
-1.7 & -104.8 & -5 & 1.4 & -0.3 & -1.5 & -1 & \\
-0.7 & -1.1 & -107.4 & 0.4 & -81e-3 & 3.1 & -0.3 & \\
32e-3 & 1.2 & 1.6 & -4.5 & 2.1 & -24e-3 & 16e-3 & 0 \\
-0.2 & -8.7 & -2 & -2.1 & -1 & 0.24 & -9e-2 & \\
80.2 & 47e2 & 984.3 & -65.9 & 16.1 & -142.7 & 47.7 & \\
\hline
3.7 & -395 & 1581.1 & -534e-4 & 8e-4 & -19e-3 & 0 &
\end{array}\right]$$

Controllers H_2 obtained via method of solution AREs [1–5].

$$K_m(s)=\left[\begin{array}{cccccccc}
548.2 & 1 & 0 & 0 & 0 & 0 & 0 & -548.3 \\
15e4 & -35 & 28e3 & 0 & 13e-4 & 0 & 0 & 15e4 \\
-19.3 & -0.4 & -288.6 & -0.5 & 14.6 & 0.5 & 61e-4 & 0 \\
-79e-4 & 0 & 0 & 0 & 0 & -0.1 & -0.1 & -3.6 \\
0 & 0 & 81.3 & 0 & -39.9 & 0 & 0 & 0 \\
-2 & 0 & 0 & 0 & 0 & -6.6 & -16.5 & -2 \\
-5.7 & 0 & 0 & 0 & 0 & 16.5 & -33.3 & -5.7 \\
\hline
0 & 0 & 449.4 & 0 & 0 & 0 & 0 & 0
\end{array}\right]$$

$$K_b(s)=\left[\begin{array}{cccccccc}
-136.8 & 1 & 0 & 0 & 0 & 0 & -1.4 & \\
-94e2 & 0 & 681.1 & 0 & 0 & 0 & -93.6 & \\
-0.7 & -0.5 & -103.1 & 176e-4 & 1e-3 & -3e-4 & 0 & \\
3e-4 & 0 & 0 & 0 & 1e-3 & 1e-3 & 39e-4 & 0 \\
-0.7 & 0 & 0 & 0 & -0.9 & -2.2 & -68e-4 & \\
-1.2 & 0 & 0 & 0 & 2.2 & -4.5 & -118e-4 & \\
\hline
0 & 0 & 1629.8 & 0 & 0 & 0 & 0 &
\end{array}\right]$$

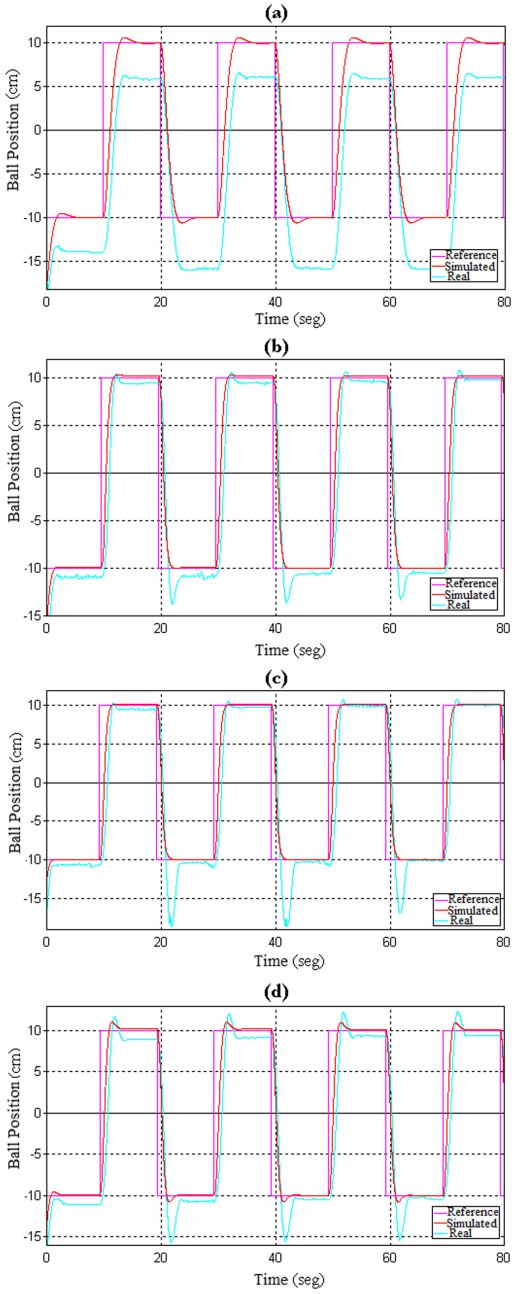


Fig. 7. Response of different closed loop systems. (a). Manufacturer's Suggested Controller RVE, (b). Controller H_∞ ARE, (c). Controller H_∞ LMI and (d). Controller H_2 ARE.

3.2 Results

Figure 7 shows the results obtained with the different controllers mentioned above. Table 3 shows the values of the main parameters that describe the response of the systems as well as the IAE performance index obtained in each case.

Table 3. Results obtained with each controller.

	RVE	H_∞ *ARE*	H_∞ *LMI*	H_2
e_{ss} (%)	41.1–65	5.17–10	6.6–5.1	10.8–8.7
t_s (sec)	4.1–4.22	3.18–3.68	3.17–3.9	3.9–3.9
SP (%)	2.3–0	4.2–38.5	2.5–87.3	16.9–58.2
IAE	1130	475.6	490.5	495.5

It is clear that the controllers H_∞ obtained by the AREs Solution Method were, in general, which present the best performance. Furthermore, the manufacturer's suggested controller is widely outperformed by each of the other drivers.

4 Conclusions

The development of this work allowed us to reach the following conclusions:

Based on previous experiences in designing robust controllers for stable plants, it was verified that an unstable plant is more difficult to control compared to a stable plant. This is basically because the presence of an unstable pole in the open-loop transfer function generally imposes a bound below the bandwidth of the closed-loop system. In other words, a rapid closed-loop system response is necessary in order not to compromise performance.

Controllers H_∞ obtained by the Solution Method of AREs offered in this case a better performance since, in general, they achieved the lowest response times, overshoot and errors in steady state, which was reflected in the fact that they presented the lowest value in the IAE performance index.

Generally robust controllers, $\boldsymbol{H_\infty}$ ***ARE***, $\boldsymbol{H_\infty}$ ***LMI***, $\boldsymbol{H_2}$ offer better performance than the design based on the classic state variable feedback technique [13, 14].

References

1. Morari, M., Zafiriou, E.: Robust Process Control. Prentice-Hall, Estados Unidos de América (1989)
2. Paganini, F.: A Course in Robust Control Theory. A Convex Approach. Springer, New York (1999)
3. Scherer, C.: Theory of Robust Control. Delft University of Technology, Delft (2001)
4. Skogestad, S., Postlethwaite, I.: Multivariable Feedback Control: Analysis and Design, Second edn. Wiley, Chichester, UK (2001)

5. Zhou, K.: Essentials of Robust Control. Prentice-Hall, New Jersey (1998)
6. Dorf, Richard C. and Bishop, Robert H.: Modern Control Systems, 10th edn. Prentice Hall (2004)
7. Quanser: SRV02-Series. Rotary Experiment # 3. Ball and Beam. User Manual
8. Quanser; SRV02-Series. Rotary Experiment # 3. Ball and Beam. Student Handout
9. Quanser: SRV02-Series. Rotary Experiment # 1. Position Control. Student Handout
10. Boyd, S., Feron, E.: Linear Matrix Inequalities in System and Control Theory. Siam, Stanford, California (1994)
11. Gahinet, P.: Explicit Controller Formulas for LMI-based H_∞ Synthesis. Automatica, vol. 32, no. 7, pp. 1007–1014. Elsevier Science Ltda, Great Britain (1995)
12. Scherer, C., Weiland, S.: Linear Matrix Inequalities in Control, 3ª Version (2000)
13. Jiménez-Cabas, J., et al.: Robust control of an evaporator through algebraic Riccati equations and D-K iteration. In: Misra, S., et al. (eds.) ICCSA 2019. LNCS, vol. 11620, pp. 731–742. Springer, Cham (2019). https://doi.org/10.1007/978-3-030-24296-1_58
14. Misra, S., et al. (eds.): ICCSA 2019. LNCS, vol. 11619. Springer, Cham (2019). https://doi.org/10.1007/978-3-030-24289-3